HHS Public Access

Author manuscript

Cardiovasc Intervent Radiol. Author manuscript; available in PMC 2019 February 05.

Published in final edited form as:

Cardiovasc Intervent Radiol. 2015 June ; 38(3): 722–730. doi:10.1007/s00270-014-1008-9.

Evaluation of a Thermoprotective Gel for Hydrodissection During Percutaneous Microwave Ablation: In Vivo Results

Anna J. Moreland,
Department of Radiology, E3/366 Clinical Science Center, University of Wisconsin – Madison, 600 Highland Avenue, Madison, WI 53792-3252, USA

Meghan G. Lubner,
Department of Radiology, E3/366 Clinical Science Center, University of Wisconsin – Madison, 600 Highland Avenue, Madison, WI 53792-3252, USA

Timothy J. Ziemlewicz,
Department of Radiology, E3/366 Clinical Science Center, University of Wisconsin – Madison, 600 Highland Avenue, Madison, WI 53792-3252, USA

Douglas R. Kitchin,
Department of Radiology, E3/366 Clinical Science Center, University of Wisconsin – Madison, 600 Highland Avenue, Madison, WI 53792-3252, USA

J. Louis Hinshaw,
Department of Radiology, E3/366 Clinical Science Center, University of Wisconsin – Madison, 600 Highland Avenue, Madison, WI 53792-3252, USA

Alexander D. Johnson,
Department of Radiology, E3/366 Clinical Science Center, University of Wisconsin – Madison, 600 Highland Avenue, Madison, WI 53792-3252, USA

Department of Biomedical Engineering, University of Wisconsin – Madison, 1111 Highland Ave, WIMR 1141, Madison, WI 53705, USA

Fred T. Lee Jr., and
Department of Radiology, E3/366 Clinical Science Center, University of Wisconsin – Madison, 600 Highland Avenue, Madison, WI 53792-3252, USA

Department of Biomedical Engineering, University of Wisconsin – Madison, 1111 Highland Ave, WIMR 1141, Madison, WI 53705, USA

Christopher L. Brace

Correspondence to: Christopher L. Brace.

Conflict of interest The MW ablation system and P407 gel used in this study incorporate aspects of multiple patents pending. No industrial support was provided for this study. Four authors of this study have affiliations with NeuWave Medical, Inc, all of which are outside the submitted work: Anna J. Moreland is a consultant; J. Louis Hinshaw is a member of the medical advisory board and shareholder; Fred T. Lee Jr. is a patent holder, member of the board of directors, and shareholder; and Christopher L. Brace is a founder, shareholder, and consultant. Meghan G. Lubner, Timothy J. Ziemlewicz, Douglas R. Kitchin, and Alexander D. Johnson have no conflict of interest.

Statement of Animal Rights All applicable institutional and/or national guidelines for the care and use of animals were followed.

Department of Radiology, E3/366 Clinical Science Center, University of Wisconsin – Madison, 600 Highland Avenue, Madison, WI 53792-3252, USA

Department of Biomedical Engineering, University of Wisconsin – Madison, 1111 Highland Ave, WIMR 1141, Madison, WI 53705, USA

Department of Medical Physics, University of Wisconsin – Madison, 1111 Highland Avenue, Room 1005, Madison, WI 53705-2275, USA

Abstract

Purpose—To evaluate whether thermoreversible poloxamer 407 15.4 % in water (P407) can protect non-target tissues adjacent to microwave (MW) ablation zones in a porcine model.

Materials and Methods—MW ablation antennas were placed percutaneously into peripheral liver, spleen, or kidney (target tissues) under US and CT guidance in five swine such that the expected ablation zones would extend into adjacent diaphragm, body wall, or bowel (non-target tissues). For experimental ablations, P407 (a hydrogel that transitions from liquid at room temperature to semi-solid at body temperature) was injected into the potential space between target and non-target tissues, and the presence of a gel barrier was verified on CT. No barrier was used for controls. MW ablation was performed at 65 W for 5 min. Thermal damage to target and non-target tissues was evaluated at dissection.

Results—Antennas were placed 7 ± 3 mm from the organ surface for both control and gel-protected ablations ($p = 0.95$). The volume of gel deployed was 49 ± 27 mL, resulting in a barrier thickness of 0.8 ± 0.5 cm. Ablations extended into non-target tissues in 12/14 control ablations (mean surface area = 3.8 cm^2) but only 4/14 gel-protected ablations (mean surface area = 0.2 cm^2; $p = 0.0005$). The gel barrier remained stable at the injection site throughout power delivery.

Conclusion—When used as a hydrodissection material, P407 protected non-targeted tissues and was successfully maintained at the injection site for the duration of power application. Continued investigations to aid clinical translation appear warranted.

Keywords

Interventional oncology; Non-vascular interventions; Ablation

Introduction

Percutaneous thermal ablation is an increasingly accepted modality to treat medically or surgically inoperable tumors of the liver, kidney, lung, and bone. In recent years, several strategies have been introduced to increase the size of ablation zones and thus achieve larger ablative margins and decrease local tumor progression [31]. Technological improvements in radiofrequency (RF) ablation include saline infusion during tissue heating [10], multiple mono-polar or bipolar switched electrodes [3, 11], higher power devices [2], and deployable electrodes with larger diameter arrays [6, 29]. Microwave (MW) ablation has seen the introduction of higher power devices [13, 25], antenna shaft cooling with water and carbon dioxide [22], antennas matched to specific tissue permittivities [8], and multiple antenna

arrays to create large and spherical ablation zones [20, 26]. Large ablation zones can also be created during percutaneous cryoablation through the use of multiple cryoprobes [34].

The larger ablation zones possible with modern ablation devices have prompted concerns about the potential for unwanted collateral damage to nearby structures. In an attempt to minimize complications, concurrent tissue displacement strategies have become standard in clinical practice. The most commonly employed technique is the injection of fluid (5 % dextrose in water [D5W, with any modality] or 0.9 % saline [NS not compatible with RF due to ionization]) [5, 9], but other methods include instillation of air or carbon dioxide [15, 18], displacement balloons [33], and leveraging the ablation zone away from vulnerable structures using the antenna itself [27].

The most important limitation when using D5W or NS to protect vulnerable structures is that fluid can move away from the injection site along paths of low mechanical resistance. This is particularly problematic for intraperitoneal fluid, which readily flows into dependent areas such as the pelvis and paracolic gutters. Therefore, an ideal thermoprotective material would be percutaneously injectable, provide adequate thermal protection, demonstrate bio-compatibility, and absorb within a finite period of time. In addition, the material should remain at or near the injection site and maintain sufficient displacement of vulnerable structures during tissue heating or cooling.

Recently, thermoreversible poloxamer 407 (P407) was introduced as a material for thermoprotection during ablation procedures [17]. P407 is a polyethylene oxide-polypropylene oxide-polyethylene oxide (PEO-PPO-PEO) triblock copolymer under active preclinical exploration for various applications [23, 36]. At certain concentrations, P407 has the unique property of existing as a liquid at or below room temperature, while organizing into a semi-solid gel at elevated (physiologic) temperatures. Thus, the material can be injected through a small-gage needle as a liquid, but solidifies once deployed within the body. Ex vivo investigation of P407 has supported use of the material for thermal protection during RF and MW ablation and suggested a lower thermal diffusivity for P407 as compared to conventional hydrodissection fluids [17]. The purpose of this study was to determine whether P407 gel can protect the diaphragm, body wall, and bowel adjacent to large microwave ablation zones in an in vivo pig model.

Materials and Methods

Poloxamer 407

P407 (Sigma Aldrich, St. Louis, MO) hydrogel was prepared using the cold method described by Schmolka et al. [30] in a 15.4 % (w/w) solution in deionized water with 2 % (v/v) iohexol (Omnipaque 300 mg/mL, General Electric, Waukesha, WI). This concentration was selected for its previously-established phase transition occurring between ambient and body temperatures (sol–gel temperature of 32 °C), thermoprotective profile adjacent to microwave ablation zones, and imaging characteristics on CT and US [17]. To aid visualization of gel at necropsy in this experiment, the P407 solution was doped with 0.5 % (v/v) India ink.

Animal Care

The experimental protocol used in this study was approved by the institutional animal care and use committee and compliant with the National Institutes of Health Guide for Care and Use of Laboratory Animals [16]. Five female domestic swine (Arlington Farms, Arlington, WI) were sedated with 7 mg/kg of intramuscular tiletamine hydrochloride plus zolazepam hydrochloride (Telazol, Wyeth, New York City, NY) and 2.2 mg/kg of xylazine hydrochloride (Xyla-Ject, Phoenix Pharmaceuticals, Burlingame, CA). Endotracheal intubation was facilitated with 0.05 mg/kg atropine, and general anesthesia was maintained with inhaled isoflurane (Halocarbon Laboratories, River Edge, NJ). At experimental conclusion, euthanasia was achieved via intravenous overdose of pentobarbital sodium and phenytoin sodium (Beuthanasia-D; Schering-Plough, Kenilworth, NJ).

MW Ablations and Placement of P407

All procedures were planned and performed by one of three board-certified radiologists with extensive clinical experience in tumor ablation (17, 6, and 4 years). MW antennas were placed percutaneously under US (Siemens Sonoline Antares, Malvern, PA) and CT (750 HD, General Electric, Waukesha, WI) guidance. Antennas were intentionally placed into positions within the peripheral liver, spleen, or kidney (target tissues) such that the expected ablation zones would extend into adjacent diaphragm, body wall, or bowel (non-target tissues). A total of 28 ablations (14 gel-protected, 14 controls) were performed in the liver (n = 10), spleen (n = 4), or kidney (n = 14) of five animals. All ablations were paired: one gel-protected ablation and one control were placed in the same organ for each animal, but distanced from each other (i.e., different liver lobes, contralateral kidney, or opposite renal pole) to avoid any overlap of the ablations.

For the experimental group, P407 was injected percutaneously through a 19-gage needle into the space between target and non-target tissues at a rate of approximately 0.33 mL/s to allow a sol–gel transition to occur at the injection site. The formation of a gel barrier between target and non-target tissues was verified by CT prior to ablation, with a target barrier thickness of 0.8 cm based on previous ex vivo experiments [17]. No barrier was used for controls.

Ablation was performed using a clinical 2.45 GHz MW ablation system (Certus 140, NeuWave Medical, Inc., Madison, WI) with a single, 15-cm, PR-type antenna (NeuWave Medical, Inc., Madison, WI) at 65 W for 5 min. Intravenous contrast-enhanced CT (120 kV, 150 mA, 1.25 mm section thickness, 45 s delays) was performed after completion of all ablations just prior to euthanasia for depiction of ablation zones, qualitative depiction of any persistent gel, and to locate positions of surrounding vulnerable structures relative to the ablation zones.

Gross Pathology

Necropsy of each animal was performed to allow for examination and *en bloc* excision of regions of thermal damage to target and non-target tissues. Diaphragm, body wall, and bowel adjacent to ablations were thoroughly inspected to evaluate for ablation extension into non-target tissue. To account for bowel motility within the peritoneal cavity (both

physiologic and during dissection), the entire bowel was examined to identify any damage. Areas of ablative damage to target and non-target tissue surfaces were documented photographically. Delineation of thermal tissue injury on gross exam was corroborated using a nitroblue tetrazolium histologic viability stain (MP Biomedicals, Santa Ana, CA) at 100 mg/100 mL prepared with Sorenson phosphate buffer to pH 7.4 as previously described by Knavel et al. [19].

Data Analysis

The surface areas of ablation zones as photographed at the interface between target and non-target organs were manually segmented using free software (ImageJ; National Institutes of Health, Bethesda, MD). Distances from antenna emission points to target organ surfaces, relative attenuation of P407, gel barrier thicknesses, and maximum axial ablation zone diameters were measured in a free DICOM reader (OsiriX, Geneva, Switzerland). The distance from the antenna emission point to the target organ surface was defined by identifying the MW antenna tip on CT axial imaging, measuring 1 cm proximal to the tip to identify the antenna emission point, and then measuring the shortest distance to the target tissue surface on the axial section capturing the emission point. Gel barrier thickness was measured in this same axial section and was defined as the gel thickness along the shortest distance from the antenna emission point to the adjacent non-target tissue. The relative attenuation of P407 was also measured in this axial section: the gel barrier in this section was manually segmented as a region of interest, and the average attenuation within the encompassed region was calculated in OsiriX using default settings. Maximum axial ablation zone diameter was measured on IV contrast-enhanced CT performed at the end of each animal experiment, with the ablation zone defined based on lack of enhancement.

Statistical Analysis

Descriptive statistics were generated for each metric (emission point distance from target tissue surface, volume of P407 delivered, gel barrier thickness, P407 attenuation on CT, maximum axial ablation zone diameter, and surface areas of ablation zones on apposed target and non-target tissues). Comparisons between control and gel-protected ablation zones were performed using a post hoc Fisher's exact test for categorical variables (presence/absence of non-target organ thermal damage) and two-tailed Wilcoxon matched pairs or Mann–Whitney tests for continuous variables (all others). p values of less than 0.05 were considered statistically significant. All statistical analyses were performed in GraphPad Prism (San Diego, CA).

Results

Overview

A summary of results from this study can be found in Table 1.

Antenna Placement

Antennas were placed with the emission point positioned at a mean of 7 mm (range: 2–13 mm) from the target organ surface for both control and gel-protected ablations ($p = 0.95$) (Fig. 1). This placed all of the emission points within range to generate ablations extending

into adjacent non-target tissue according to manufacturer-established time and power guidelines.

P407 Placement

The mean (± standard deviation) volume of gel deployed between the target and non-target tissue was 49.3 ± 27.2 mL, resulting in a gel barrier thickness of 7.5 ± 4.8 mm. Notably, under US guidance, P407 demonstrated transient fluid-like behavior post-injection, which allowed for interspersion into complex anatomic spaces (Fig. 2). A transition to semi-solid behavior was noted on the order of seconds after injection.

CT Documentation of Completed Ablations

Non-contrast CT performed at the conclusion of each ablation demonstrated that the gel remained stable in position throughout power delivery (Fig. 3). Although not a primary endpoint of this study, absorption of gel from early ablations and accumulation of contrast in the bladder was incidentally observed by 2.5 h post initial introduction of iohexol-doped P407. Intravenous contrast-enhanced CT was performed after completion of all ablations just prior to euthanasia, and demonstrated ablation zone maximum axial diameters of 3.3 ± 0.9 cm for control ablations and 3.8 ± 1.2 cm for gel-protected ablations ($p = 0.3$).

Gross Pathology

At the time of necropsy, in situ gel was only transiently observable, as the P407 returned to the liquid phase once laparotomy was performed and the material returned to room temperature (Fig. 4). Examination at necropsy allowed for identification of ablation zones at the target organ surface for 14/14 ablations. There was no difference in the surface area of control ablations compared to gel-protected ablations (6.8 ± 4.0 and 7.1 ± 3.8 cm^2, respectively; $p = 1.0$).

Ablations extended into non-target tissues in 12/14 control ablations but only 4/14 gel-protected ablations ($p = 0.006$). In addition, the extent of thermal damage to non-target tissues was significantly greater adjacent to control ablations than gel-protected ablations (3.8 ± 3.7 cm^2 versus 0.2 ± 0.5 cm^2, respectively; $p = 0.0005$). When comparing just the ablations in which there was damage to non-target tissue present, the extent of thermal damage was greater adjacent to control ablations than gel-protected ablations, but this trend did not reach statistical significance (4.4 ± 3.6 cm^2 versus 0.8 ± 0.6 cm^2, respectively; $p = 0.0602$). Retrospective analysis after review of gross pathology results revealed that the mean gel thickness in cases where ablations did not extend to non-target tissues was 0.8 ± 0.5 cm, while thickness among ablations that extended into non-target tissues was 0.6 ± 0.3 cm ($p = 0.5$) (Fig. 5).

Discussion

The results of this study suggest that P407 exhibits potential as an effective thermoprotective barrier during high-powered microwave ablation. The gel remained at the injection site before and during ablation, provided excellent protection to non-target organs, and appeared to absorb after several hours. It should be noted that this experiment was a far more extreme

test than what would be expected in most clinical situations. The emission points of the microwave antennas were placed very close to adjacent non-target organs (mean < 1 cm) such that damage to these tissues was considered inevitable without protection. Despite these conditions, the gel barrier protected non-target organs: if there was damage to adjacent gel-protected structures, it was minimal, and if gel barriers were sufficiently thick, there was no damage discernable. As was previously shown ex vivo, a barrier thickness of at least 0.8 cm provided the most effective insulation against a typical power delivery cycle with this high-powered MW ablation device [17].

In vitro and ex vivo comparison of conventional hydro-dissection fluids versus P407 has suggested that there may be fundamental differences in their thermal properties leading to differing mechanisms of thermoprotection during percutaneous ablation [17]. Free convection of conventional hydrodissection fluids (D5W, NS) appears to account for the majority of their heat dissipation. In contrast, this appears to play little to no role in the mechanism of P407 given its semi-solid phase. Instead, it appears to work primarily through conductive heat dissipation and is also hypothesized to have an inherently low thermal diffusivity. Further studies to characterize the mechanisms of thermoprotection for both conventional fluids and P407 are ongoing.

A number of complications associated with thermal ablation techniques are secondary to thermal damage to non-target tissues: bowel perforation, collecting system injury, body wall and skin burns, pleural effusion, and post-procedural pain [21, 24, 35]. By achieving displacement and thermal protection of adjacent structures, P407 could mitigate tumor proximity to vulnerable structures as a contraindication to ablation. Thermal protection of adjacent structures could also allow operators to adopt more aggressive strategies to generate larger ablation zones. The ability to safely generate larger ablation zones, in turn, could enable ablation of larger tumors and improvement of ablative margins with the goal of decreasing rates of local tumor progression.

By far, the most common strategies for protection of vulnerable structures in practice today are hydrodissection with NS or D5W [5, 9]. The low viscosities of NS and D5W pose a challenge during hydrodissection due to their tendency to flow away from the injection site into dependent locations such as the pelvis or paracolic gutters. In some cases, this phenomenon cannot be overcome, and displaced tissues reappose after fluids diffuse away. In other scenarios, displacement can be maintained via continuous injection of fluid for the duration of the ablation. Maintaining such a barrier can require multiple liters of fluid [1, 14], which can be problematic in patients susceptible to volume overload and often results in marked patient discomfort from distention. P407 shares the property of low viscosity at room temperature with NS and D5W, which allows for injection through small needles. However, P407 transitions within seconds to a more stable, semi-solid state at body temperature, providing for targeted injection and a stable thermal barrier.

Previous in vitro characterization of P407 noted that the gel phase melted above 55 °C [17]. Such temperatures are certainly achieved during virtually all microwave ablation cases. However, in the present study, gel barriers were maintained during each ablation as demonstrated on post-ablation CT. Based on the previous in vitro work [17], we infer that a

layer of melted P407 develops closest to the antenna, and that the remainder of the gel barrier remains at temperatures low enough to remain as a semi-solid.

Hyaluronic acid has also been employed as a thermo-protective gel for tissue hydrodissection [12]. Hyaluronic acid offers the advantage of having a long track record for clinical use, with well-characterized biocompatability in humans. However, parallel investigation into the use of P407 as a hydrodissection material is warranted for several reasons: hyaluronic acid has been studied for use during RF but not MW ablation, it appears to persist in body cavities for days whereas P407 is reabsorbed over hours, and it does not demonstrate a phase change to liquid at ambient temperatures. To the last point, initial results suggest that hyaluronic acid's viscosity did not limit percutaneous injectability of the material. However, as illustrated in this study, the sol–gel transition behavior of P407 could present distinct advantages by allowing for dispersion into complex spaces in the liquid state before solidifying into gel form.

There were several limitations to the present study. The sample size was relatively small (n = 28 ablations) and a variety of organs were used to minimize the number of animals that were sacrificed. However, the sample size was large enough to achieve statistical significance for the primary endpoints of the study. The use of a normal porcine model rather than a tumor model likely had no effect on the main conclusions of the study, which revolve around thermoprotection rather than treatment effectiveness. The use of a single microwave system was also unlikely to affect the results of the study, and the choice of MW system was only important for the ability make ablation zones large enough to extend into and damage adjacent organs without thermoprotection. Comparison was not made between P407 and conventional hydrodissection fluids, although prior studies have characterized differences in thermoprotection between the materials in more controlled in vitro and ex vivo settings [17]. As mentioned previously, the close proximity of ablations to vulnerable tissues (mean distance from emission point to non-target tissue = 7 mm) represented an extreme scenario not likely to be attempted in a clinical setting. Ongoing studies are underway to characterize P407's pharmacologic properties, but previous work indicates it has weak immunogenicity and low toxicity [7, 32]. Human studies to characterize the safety, pharmacodynamics, and pharmacokinetics of intraperitoneal P407 have not yet been performed, but animal studies suggest that intraperitoneal injections of P407 have a half life of approximately 21 h based on urinary excretion [28]. P407 is currently Food and Drug Administration-approved for clinical use in vascular anastomosis [4] and is under active preclinical investigation for many additional novel applications [23, 36].

In conclusion, the results of this study suggest that percutaneous delivery of P407 for tissue hydrodissection is technically feasible, forms a barrier that is maintained during a typical microwave ablation, and confers thermoprotection of structures adjacent to ablation targets in an animal model. Further comparison of P407 to existing hydrodissection fluids, evaluation for use in RF and cryoablation, and continued investigations into pharmacokinetic/pharmacodynamic properties for intraperitoneal use appear warranted.

Acknowledgments

The authors thank Lisa Sampson, M.S.; Alice Minx, B.Sc.; Thomas Warner, M.D., and Jeffrey Wu for their help with experimental setup.

Funding Sources NIH R01CA142737, R01CA149379; Wisconsin Alumni Research Foundation Technology Development program.

References

1. Bodily KD, Atwell TD, Mandrekar JN et al. (2010) Hydrodis-placement in the percutaneous cryoablation of 50 renal tumors. AJR Am J Roentgenol 194(3):779–783 [PubMed: 20173159]
2. Brace CL, Laeseke PF, Sampson LA, Frey TM, Mukherjee R, Lee FT, Jr (2007) Radiofrequency ablation with a high-power generator: device efficacy in an in vivo porcine liver model. Int J Hyperth 23(4):387–394
3. Brace CL, Sampson LA, Hinshaw JL, Sandhu N, Lee FT, Jr (2009) Radiofrequency ablation: simultaneous application of multiple electrodes via switching creates larger, more confluent ablations than sequential application in a large animal model. J Vasc Interv Radiol 20(1):118–124 [PubMed: 19019701]
4. Chang EI, Galvez MG, Glotzbach JP et al. (2011) Vascular anastomosis using controlled phase transitions in poloxamer gels. Nat Med 17(9):1147–1152 [PubMed: 21873986]
5. Chen EA, Neeman Z, Lee FT, Kam A, Wood B (2006) Thermal protection with 5 % dextrose solution blanket during radiofrequency ablation. Cardiovasc Interv Radiol 29(6):1093–1096
6. Clark TW, Malkowicz B, Stavropoulos SW et al. (2006) Radio-frequency ablation of small renal cell carcinomas using multi-tined expandable electrodes: preliminary experience. J Vasc Interv Radiol 17(3):513–519 [PubMed: 16567676]
7. Dumortier G, Grossiord JL, Agnely F, Chaumeil JC (2006) A review of poloxamer 407 pharmaceutical and pharmacological characteristics. Pharm Res 23(12):2709–2728 [PubMed: 17096184]
8. Durick NA, Laeseke PF, Broderick LS et al. (2008) Microwave ablation with triaxial antennas tuned for lung: results in an in vivo porcine model. Radiology 247(1):80–87 [PubMed: 18292471]
9. Farrell MA, Charboneau JW, Callstrom MR, Reading CC, Engen DE, Blute ML (2003) Paranephric water instillation: a technique to prevent bowel injury during percutaneous renal radiofrequency ablation. AJR Am J Roentgenol 181(5):1315–1317 [PubMed: 14573426]
10. Goldberg SN, Ahmed M, Gazelle GS et al. (2001) Radio-frequency thermal ablation with NaCl solution injection: effect of electrical conductivity on tissue heating and coagulation-phantom and porcine liver study. Radiology 219(1):157–165 [PubMed: 11274551]
11. Haemmerich D, Staelin ST, Tungjitkusolmun S, Lee FT, Jr, Mahvi DM, Webster JG (2001) Hepatic bipolar radio-frequency ablation between separated multiprong electrodes. IEEE Trans Bio-med Eng 48(10):1145–1152
12. Hasegawa T, Takaki H, Miyagi H et al. (2013) Hyaluronic acid gel injection to prevent thermal injury of adjacent gastrointestinal tract during percutaneous liver radiofrequency ablation. Cardiovasc Interv Radiol 36(4):1144–1146
13. Hines-Peralta AU, Pirani N, Clegg P et al. (2006) Microwave ablation: results with a 2.45-GHz applicator in ex vivo bovine and in vivo porcine liver. Radiology 239(1):94–102 [PubMed: 16484351]
14. Hinshaw JL, Laeseke PF, Winter TC, 3rd, Kliewer MA, Fine JP, Lee FT, Jr (2006) Radiofrequency ablation of peripheral liver tumors: intraperitoneal 5 % dextrose in water decreases post-procedural pain. AJR Am J Roentgenol 186(5 Suppl):S306–S310 [PubMed: 16632692]
15. Hiraki T, Gobara H, Shibamoto K et al. (2011) Technique for creation of artificial pneumothorax for pain relief during radio-frequency ablation of peripheral lung tumors: report of seven cases. J Vasc Interv Radiol 22(4):503–506 [PubMed: 21354819]
16. Institute of Laboratory Animal Resources CoLS, National Research Council (1996) Guide for the care and use of laboratory animals. National Academy Press, Washington, DC

17. Johnson A, Sprangers A, Cassidy P et al. (2013) Design and validation of a thermoreversible material for percutaneous tissue hydrodissection. Journal of biomedical materials research Part B
18. Kamusella P, Wiggermann P, Wissgott C, Andresen R, Stroszczynski C (2011) Thermal protection of targeted air instillation in CT-guided radiofrequency ablation. RoFo : Fortschritte auf dem Gebiete der Rontgenstrahlen und der Nuklearmedizin 183(10):952–955 [PubMed: 21748697]
19. Knavel EM, Hinshaw JL, Lubner MG et al. (2012) High-powered gas-cooled microwave ablation: shaft cooling creates an effective stick function without altering the ablation zone. AJR Am J Roentgenol 198(3):W260–W265 [PubMed: 22358023]
20. Laeseke PF, Lee FT, Jr, van der Weide DW, Brace CL (2009) Multiple-antenna microwave ablation: spatially distributing power improves thermal profiles and reduces invasiveness. J Interv Oncol 2(2):65–72 [PubMed: 21857888]
21. Liang P, Wang Y, Yu X, Dong B (2009) Malignant liver tumors: treatment with percutaneous microwave ablation–complications among cohort of 1,136 patients. Radiology 251(3):933–940 [PubMed: 19304921]
22. Liang P, Yu J, Yu XL et al. (2012) Percutaneous cooled-tip microwave ablation under ultrasound guidance for primary liver cancer: a multicentre analysis of 1,363 treatment-naive lesions in 1,007 patients in China. Gut 61(7):1100–1101 [PubMed: 21997552]
23. Lin T, Wu J, Zhao X et al. (2014) In situ floating hydrogel for intravesical delivery of adriamycin without blocking urinary tract. J Pharm Sci 103(3):927–936 [PubMed: 24449076]
24. Livraghi T, Meloni F, Solbiati L, Zanus G, Collaborative Italian Group using As (2012) Complications of microwave ablation for liver tumors: results of a multicenter study. Cardiovasc Interv Radiol 35(4):868–874
25. Lubner MG, Hinshaw JL, Andreano A, Sampson L, Lee FT, Jr, Brace CL (2012) High-powered microwave ablation with a small-gauge, gas-cooled antenna: initial ex vivo and in vivo results. J Vasc Interv Radiol 23(3):405–411 [PubMed: 22277272]
26. Oshima F, Yamakado K, Nakatsuka A, Takaki H, Makita M, Takeda K (2008) Simultaneous microwave ablation using multiple antennas in explanted bovine livers: relationship between ablative zone and antenna. Radiat Med 26(7):408–414 [PubMed: 18769998]
27. Park BK, Kim CK (2008) Using an electrode as a lever to increase the distance between renal cell carcinoma and bowel during CT-guided radiofrequency ablation. Eur Radiol 18(4): 743–746 [PubMed: 18060410]
28. Pec EA, Wout ZG, Johnston TP (1992) Biological activity of urease formulated in poloxamer 407 after intraperitoneal injection in the rat. J Pharm Sci 81(7):626–630 [PubMed: 1403693]
29. Rossi S, Buscarini E, Garbagnati F et al. (1998) Percutaneous treatment of small hepatic tumors by an expandable RF needle electrode. AJR Am J Roentgenol 170(4):1015–1022 [PubMed: 9530052]
30. Schmolka IR, Schmolka IR (1972) Artificial skin. I. Preparation and properties of pluronic F-127 gels for treatment of burns. J Biomed Mater Res 6(6):571–582 [PubMed: 4642986]
31. Shyn PB, Mauri G, Alencar RO et al. (2014) Percutaneous imaging-guided cryoablation of liver tumors: predicting local progression on 24-hour MRI. AJR, American journal of roentgenology
32. Singh-Joy SD, McLain VC (2008) Safety assessment of poloxamers 101, 105, 108, 122, 123, 124, 181, 182, 183, 184, 185, 188, 212, 215, 217, 231, 234, 235, 237, 238, 282, 284, 288, 331, 333, 334, 335, 338, 401, 402, 403, and 407, poloxamer 105 benzoate, and poloxamer 182 dibenzoate as used in cosmetics. Int J Toxicol 27(Suppl 2):93–128 [PubMed: 18830866]
33. Yamakado K, Nakatsuka A, Akeboshi M, Takeda K (2003) Percutaneous radiofrequency ablation of liver neoplasms adjacent to the gastrointestinal tract after balloon catheter interposition. J Vasc Interv Radiol 14(9 Pt 1):1183–1186 [PubMed: 14514811]
34. Young JL, McCormick DW, Kolla SB et al. (2012) Are multiple cryoprobes additive or synergistic in renal cryotherapy? Urology 79(2):484 e481–484 e486
35. Yu J, Liang P, Yu XL et al. (2014) US-guided percutaneous microwave ablation versus open radical nephrectomy for small renal cell carcinoma: intermediate-term results. Radiology 270(3):880–887 [PubMed: 24475805]
36. Zhao YZ, Lv HF, Lu CT et al. (2013) Evaluation of a novel thermosensitive heparin-poloxamer hydrogel for improving vascular anastomosis quality and safety in a rabbit model. PLoS ONE 8(8):e73178 [PubMed: 24015296]

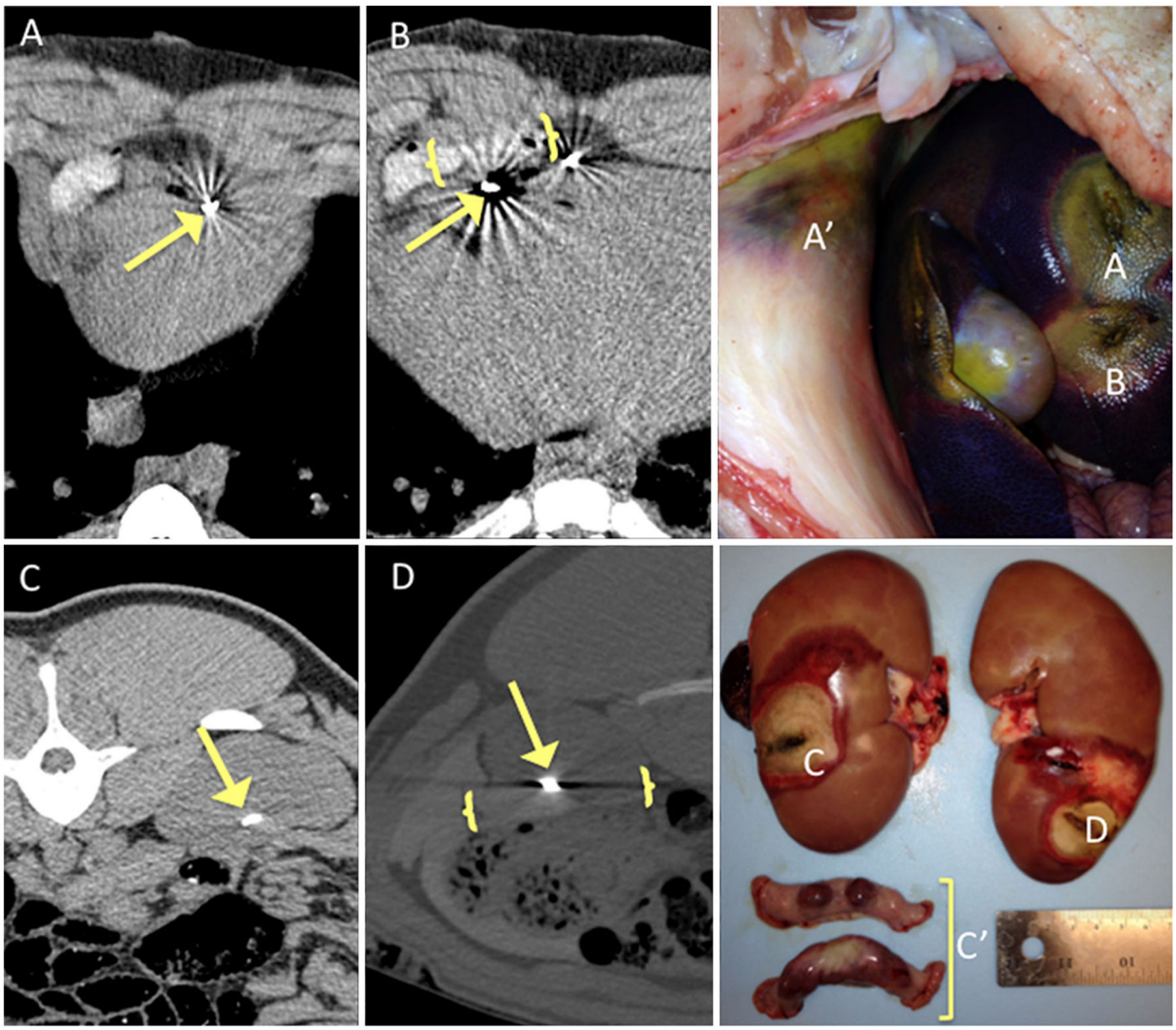

Fig. 1.

Antenna/gel placement and gross appearance of microwave ablations without and with poloxamer 407 hydrodissection of non-target structures in a swine model. Antenna emission points indicated by *arrows, gel barrier bracketed* on CT images. Ablation of peripheral liver (**A**) demonstrates extension into diaphragm (**A′**) without gel, while gel-protected liver ablation (**B**) does not extend into diaphragm on in situ gross photograph. Ablation of anterior kidney (**C**) demonstrates extension into bowel (**C′**) without gel. No bowel damage was noted adjacent to the gel-protected kidney ablation (**D**)

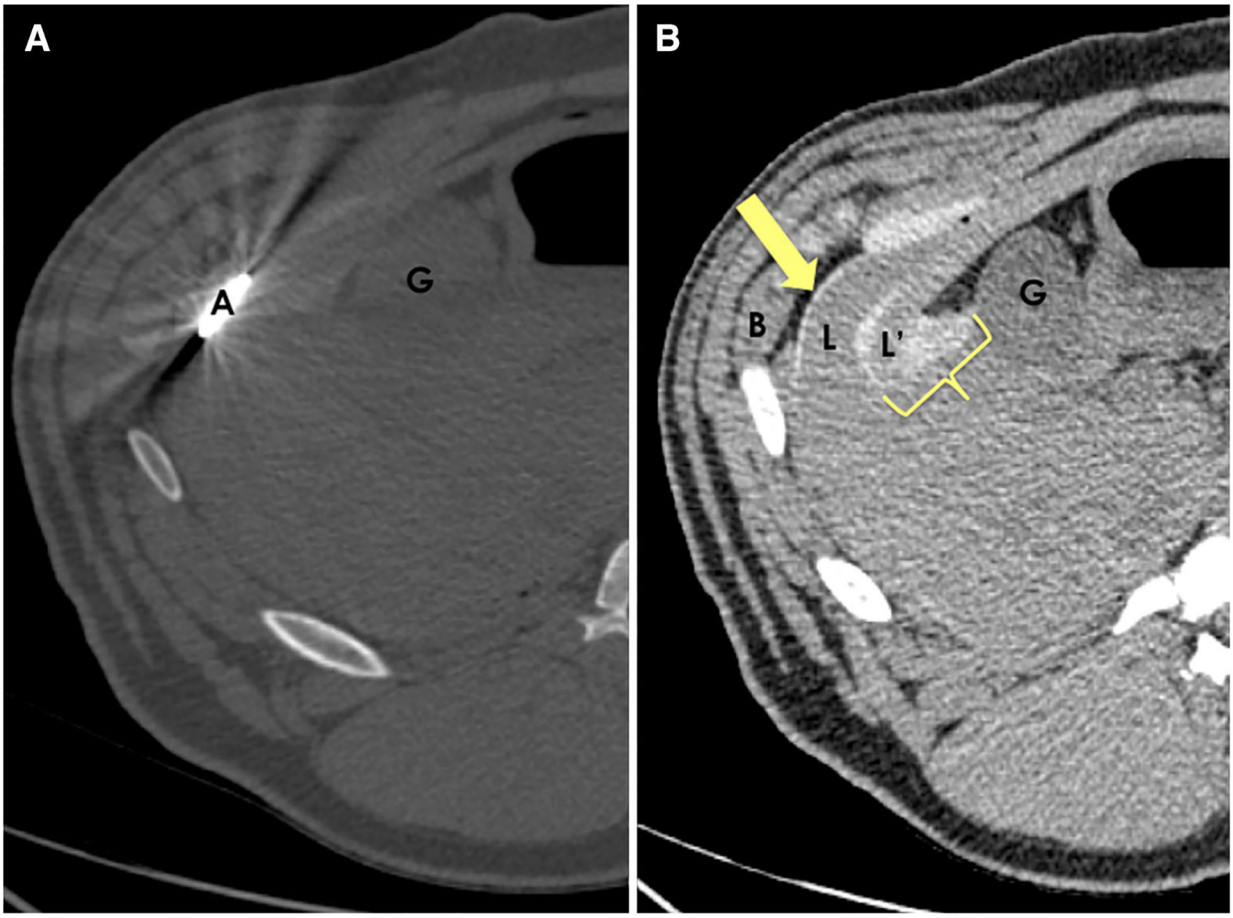

Fig. 2.

P407 placement within a complex space to protect multiple non-target tissues simultaneously. (***A***) MW antenna placement and (***B***) slightly inferior axial CT slice with less streak artifact to better depict anatomy. Antenna (*A*) was placed within the target tissue: in this case, the most lateral portion of the liver (*L*). Body wall (*B*), another lobe of the liver (*L*′), and the gallbladder (*G*) were all in close proximity to the desired ablation site. Percutaneous injection of P407 allowed for formation of a gel barrier between the target liver lobe and the body wall (*arrow*), as well as a barrier enveloping the second liver lobe and abutting the gallbladder (*bracket*)

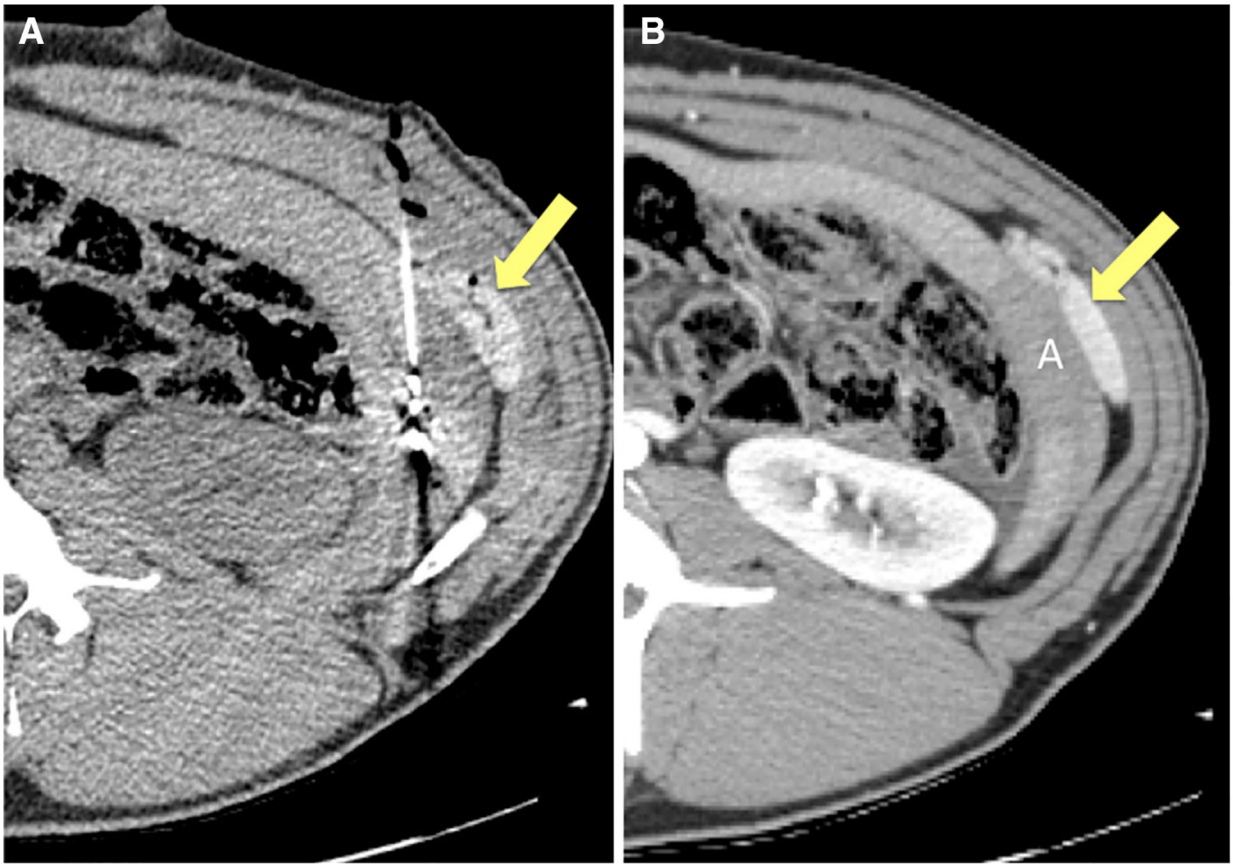

Fig. 3.

P407 gel position maintenance throughout MW ablation. P407 barrier (*arrow*) placement between MW antenna emission point within spleen and the body wall on non-contrast CT (**A**) and intravenous contrast-enhanced CT performed 2 h later (**B**) demonstrating completed ablation zone (*A*) and stable position of gel barrier (*arrow*)

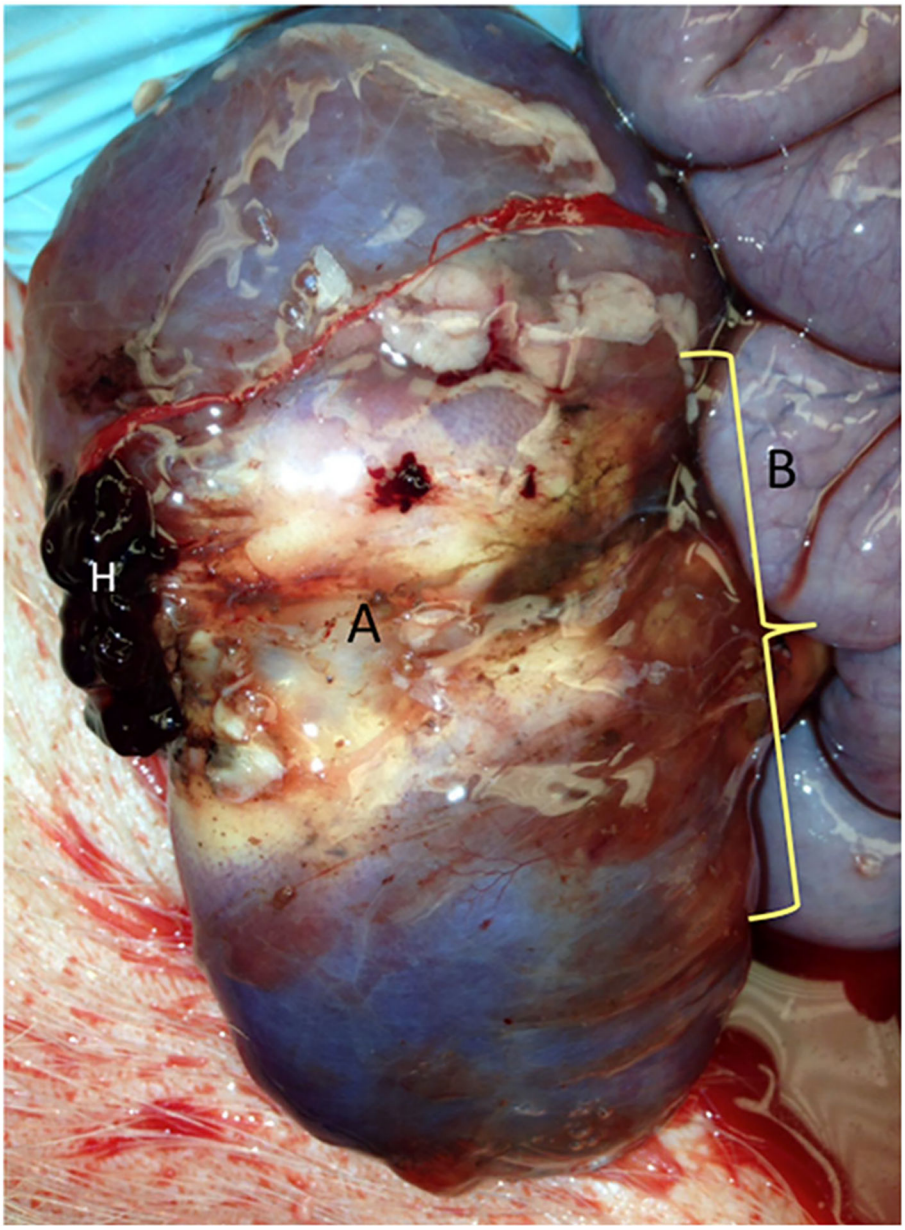

Fig. 4.

In situ P407 gel barrier after MW ablation. P407 rapidly changed phase to liquid form after laparotomy at exposure to ambient temperatures. However, this image was captured immediately after dissection into the retroperitoneum and depicts a rapidly liquefying gel barrier (*bracketed*, translucent substance tinted with India ink) that persisted through necropsy in this protected space between a MW ablation in the kidney (*A*) and adjacent bowel (*B*). Note that this particular ablation was intentionally placed within the hilum and resulted in the ischemic appearance of the kidney in this image. *H* represents a small hematoma adherent to the kidney capsule

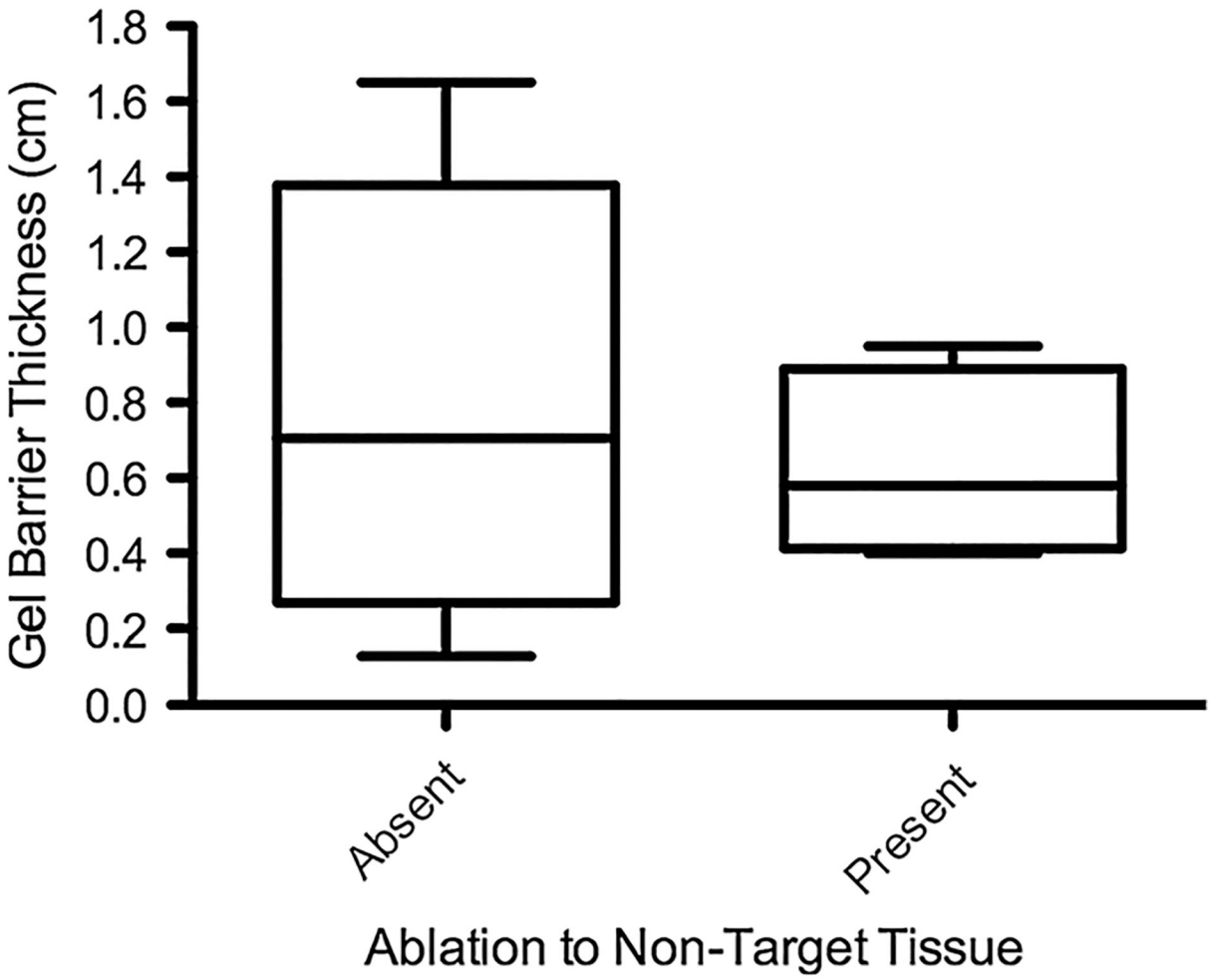

Fig. 5.

Comparison of P407 barrier thickness for gel-protected ablations without ($n = 10$) and with ($n = 4$) ablation extension to non-target tissue. Boxes represent mean (0.8 and 0.6 cm, respectively) ± SEM, whiskers represent range, $p = 0.5$

Table 1

Results of control and P407-protected ablations

	Control ablations	Gel-protected ablations	*p* value
Number of ablations (*n*)	14	14	
Distance from antenna emission point to target organ surface (cm)			
Mean (SD)	0.7 (0.3)	0.7 (0.4)	0.95
Range	0.2–1.3	0.1–1.6	
Ablation zone maximum axial diameter (cm)			
Mean (SD)	3.3 (0.9)	3.8 (1.2)	0.3
Ablation zone area on target organ surface (cm^2)			
Mean (SD)	6.8 (4.0)	7.1 (3.8)	1.0
Volume P407 (mL)			
Mean (SD)	0 (0)	49 (27)	
Range		30–120	
P407 barrier thickness (cm)			
Mean (SD)	0 (0)	0.8 (0.5)	
Range		0.13–1.65	
P407 CT attenuation (HU)			
Mean (SD)		114 (11)	
Range		93–140	
Number of ablations extending to non-target tissue, n (%)	12 (85.7)	4 (28.6)	0.006
Ablation zone area on non-target organ surface (cm^2)			
Mean (SD)	3.8 (3.7)	0.2 (0.5)	0.0005
Range	0–10.1	0–1.4	